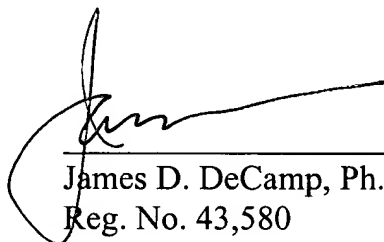## CONCLUSION

Applicants submit that the pending claims are in condition for allowance and such action is respectfully requested. If the Office does not concur, an interview with the undersigned is hereby requested.

Enclosed is a Petition to extend the period for filing an Appeal Brief for five months, to and including February 22, 2005.

If there are any additional charges or any credits, please apply them to Deposit Account No. 03-2095.

Respectfully submitted,

Date: _22 February 2005_

James D. DeCamp, Ph.D.
Reg. No. 43,580

Clark & Elbing LLP
101 Federal Street
Boston, MA 02110
Telephone: 617-428-0200
Facsimile: 617-428-7045

surface of the antennal lobes through a small window cut in the head cuticle; these experiments were done without the experimenter knowing whether the drop contained PCT or saline. In the second method (group 2, Table 1), 0.1 nl saline or picrotoxin (100 μM–1 mM in saline) was injected directly into the antennal lobes through a small window in the head just above the base of each antenna using a Picospritzer (General Valve)[25]. Injections gave the same results as topical applications, although PE response rates were reduced, as commonly observed after extensive surgery. After a time t_1 (10, 45, 60 or 90 min) for recovery, animals were trained by using the following protocol[13,14]: 6 paired presentations of odorant (4-s pulse into a vented air stream) and sucrose (0.4 μl of 1.25 M solution for group 1, 2 μl of 2 M solution for group 2, presented to the antenna and the proboscis 3 s after odorant pulse onset), every 2 min (group 1) or 30 s (group 2). Animals showing a PE response in each trial were selected to receive 2 or 3 extinction (odour only) trials (one with each of the 2 or 3 test odours; see below) 90 min (group 1) or 60 min (group 2) after conditioning. The odorants used for conditioning were 1-hexanol or 1-octanol. Groups were counterbalanced to contain roughly equal numbers of bees trained with either alcohol. The odours used for testing (1-octanol, 1-hexanol, geraniol) were presented to each animal in a randomized order. Generalization between the alcohols and geraniol is typically low[16]. We used the percentage of subjects that responded to an extinction test as the response measure. Results were compared with χ^2 statistics because behavioural data were categorical (PE or no PE). Statistical values are one-tailed because generalization responses were not expected to exceed the response levels to conditioned stimuli.

1. Adrian, E. D. Olfactory reactions in the brain of the hedgehog. *J. Physiol. (Lond.)* 100, 459–473 (1942).
2. Gray, C. M. & Skinner, J. E. Centrifugal regulation of neuronal activity in the olfactory bulb of the waking rabbit as revealed by reversible cryogenic blockade. *Exp. Brain Res.* 69, 378–386 (1988).
3. Gelperin, A. & Tank, D. W. Odour-modulated collective network oscillations in a terrestrial mollusc. *Nature* 345, 437–440 (1990).
4. Delaney, K. R. et al. Waves and stimulus-modulated dynamics in an oscillating olfactory network. *Proc. Natl Acad. Sci. USA* 91, 669–674 (1994).
5. Laurent, G. & Davidowitz, H. Encoding of olfactory information with oscillating neural assemblies. *Science* 265, 1872–1875 (1994).
6. Gray, C. M. & Singer, W. Stimulus specific neuronal oscillations in orientation columns of cat visual cortex. *Proc. Natl Acad. Sci. USA* 86, 1698–1702 (1989).
7. Singer, W. & Gray, C. M. Visual feature integration and the temporal correlation hypothesis. *Annu. Rev. Neurosci.* 18, 555–586 (1995).
8. Neuenschwander, S. & Varela, F. J. Visually triggered neuronal oscillations in the pigeon—an autocorrelation study of tectal activity. *Eur. J. Neurosci.* 7, 870–881 (1993).
9. Laurent, G., Wehr, M. & Davidowitz, H. Temporal representations of odors in an olfactory network. *J. Neurosci.* 16, 3837–3847 (1996).
10. Wehr, M. & Laurent, G. Temporal combinatorial encoding of odours with oscillations. *Nature* 384, 162–166 (1996).
11. Laurent, G. Dynamical representation of odors by oscillating and evolving neural assemblies. *Trends Neurosci.* 19, 489–496 (1996).
12. MacLeod, K. & Laurent, G. Distinct mechanisms for synchronization and temporal patterning of odor-encoding neural assemblies. *Science* 274, 976–979 (1996).
13. Kuwabara, M. Bildung des bedingten reflexes von pavlovs typus bei der honigbiene, *Apis mellifica. J. Fac. Sci. Hokkaido Univ. (Ser. VI Zool.)* 13, 458–464 (1957).
14. Bitterman, M. E., Menzel, R., Fietz, A. & Schäfer, S. Classical conditioning of proboscis extension in honeybees (*Apis mellifera*). *J. Comp. Psychol.* 97, 107–119 (1983).
15. Menzel, R. & Bitterman, M. E. in *Neuroethology and Behavioral Physiology* (eds Huber, F. & Markl, H.) 206–215 (Springer, New York, 1983).
16. Smith, B. H. & Menzel, R. The use of electromyogram recordings to quantify odorant discrimination in the honey bee, *Apis mellifera. J. Insect Physiol.* 35, 369–375 (1989).
17. Menzel, R. in *Neurobiology of Comparative Cognition* (eds Kesner, R. P. & Olton, D. S.) 237–292 (Erlbaum, New Jersey, 1990).
18. Menzel, R., Michelson, B., Rüffer, P. & Sugawa, M. in *Modulation of Synaptic Plasticity in Nervous Systems* NATO ASI series, Vol. H19 (eds Hertung, G. & Spatz, H.-C.) 335–350 (Springer, Berlin, 1988).
19. Yokoi, M., Mori, K. & Nakanishi, S. Refinement of odor molecule tuning by dendrodendritic synaptic inhibition in the olfactory bulb. *Proc. Natl Acad. Sci. USA* 92, 3371–3375 (1995).
20. Joerges, J., Kuttner, A., Galizia, C. G. & Menzel, R. Representation of odours and odour mixtures visualized in the honeybee brain. *Nature* 387, 285–288 (1997).
21. Murthy, V. N. & Fetz, E. E. Coherent 25 Hz to 35 Hz oscillations in the sensorimotor cortex of awake behaving monkeys. *Proc. Natl Acad. Sci. USA* 89, 5670–5674 (1992).
22. Gray, C. M. Synchronous oscillations in neuronal systems: mechanisms and functions. *J. Comput. Neurosci.* 1, 11–38 (1994).
23. Mauelshagen, J. Neural correlates of olfactory learning-paradigms in an identified neuron in the honeybee brain. *J. Neurophysiol.* 69, 609–625 (1993).
24. Bhagavan, S. & Smith, B. H. Olfactory conditioning in the honey-bee, *Apis mellifera*—effects of odor intensity. *Physiol. Behav.* 61, 107–117 (1997).
25. Smith, B. H. An analysis of blocking in binary odorant mixtures: An increase but not a decrease in intensity of reinforcement produces unblocking. *Behav. Neurosci.* 111, 57–69 (1997).
26. Macmillan, C. S. & Mercer, A. R. An investigation of the role of dopamine in the antennal lobes of the honeybee, *Apis mellifera. J. Comp. Physiol.* A 160, 359–366 (1987).

Prion (PrP^{Sc})-specific epitope defined by a monoclonal antibody

C. Korth*, B. Stierli†, P. Streit†, M. Moser*, O. Schaller*, R. Fischer‡, W. Schulz-Schaeffer§, H. Kretzschmar§, A. Raeber‖, U. Braun¶, F. Ehrensperger☆, S. Hornemann#, R. Glockshuber#, R. Riek#, M. Billeter#, K. Wüthrich# & B. Oesch*

* *Prionics AG, University of Zürich, Winterthurerstrasse 190, 8057 Zürich, Switzerland*
† *Brain Research Institute, University of Zürich, 8029 Zürich, Switzerland*
‡ *Institut für Biochemie, ETH Zürich, 8092 Zürich, Switzerland*
§ *Institut für Neuropathologie, Universität Göttingen, 37075 Göttingen, Germany*
‖ *Institut für Neuropathologie, University of Zürich, 8091 Zürich, Switzerland*
¶ *Klinik für Wiederkäuer- und Pferdemedizin, University of Zürich, 8057 Zürich, Switzerland*
☆ *Institut für Veterinärpathologie, University of Zürich, 8057 Zürich, Switzerland*
Institut für Molekularbiologie und Biophysik, ETH Zürich, 8093 Zürich, Switzerland

....

Prions are infectious particles causing transmissible spongiform encephalopathies (TSEs). They consist, at least in part, of an isoform (PrP^{Sc}) of the ubiquitous cellular prion protein (PrP^{C}). Conformational differences between PrP^{C} and PrP^{Sc} are evident from increased β-sheet content and protease resistance in PrP^{Sc} (refs 1–3). Here we describe a monoclonal antibody, 15B3, that can discriminate between the normal and disease-specific forms of PrP. Such an antibody has been long sought as it should be invaluable for characterizing the infectious particle as well as for diagnosis of TSEs such as bovine spongiform encephalopathy (BSE) or Creutzfeldt–Jakob disease (CJD) in humans. 15B3 specifically precipitates bovine, murine or human PrP^{Sc}, but not PrP^{C}, suggesting that it recognizes an epitope common to prions from different species. Using immobilized synthetic peptides, we mapped three polypeptide segments in PrP as the 15B3 epitope. In the NMR structure of recombinant mouse PrP, segments 2 and 3 of the 15B3 epitope are near neighbours in space, and segment 1 is located in a different part of the molecule. We discuss models for the PrP^{Sc}-specific epitope that ensure close spatial proximity of all three 15B3 segments, either by intermolecular contacts in oligomeric forms of the prion protein or by intramolecular rearrangement.

PrP-null mice were immunized with full-length recombinant bovine PrP. After fusion of spleen cells with myeloma cells, we selected ~50 hybridoma cells that produced monoclonal antibodies recognizing either native bovine PrP^{Sc} (PrP^{BSE}) immobilized on nitrocellulose or recombinant bovine PrP (rbPrP) in an enzyme-linked immunosorbent assay (ELISA). One of these antibodies (15B3) was selected for binding to protease-digested BSE brain homogenates; a second (6H4) efficiently recognized recombinant PrP. On western blots, 6H4 recognized rbPrP, as well as bovine, human, mouse and sheep PrP^{C}, whereas 15B3 did not react with any form of PrP (results not shown). To determine the reactivity of these antibodies with native PrP^{C} and PrP^{Sc}, we immunoprecipitated PrP from brain homogenates of normal and BSE-infected cattle. The precipitated proteins were then analysed on western blots using a rabbit polyclonal antiserum to rbPrP (Fig. 1). The 6H4 antibody precipitated PrP from BSE as well as from normal brain homogenates; 15B3 precipitated only PrP from brain homogenates of BSE-diagnosed cattle (Fig. 1a). Upon proteinase K treatment, normal PrP is completely digested, whereas the 33K–35K form of PrP^{Sc} is shortened to 27K–30K (PrP 27–30), probably as a result of

degradation of the amino-terminal segment of residues 23–90, analogous to hamster PrP^{Sc} (ref. 3). Digestions of brain homogenates or immunoprecipitates with proteinase K are shown in Fig. 1b. Proteinase K digestion of BSE homogenates or the immunoprecipitate with 15B3 yields the PrP^{BSE}-specific band of 27K–30K (Fig. 1b). Not all of the immunoprecipitated PrP was protease-resistant, suggesting that 15B3 recognizes multiple forms of disease-specific PrP with different sensitivities to proteinase K. Apparently, PrP with properties characteristic for PrP^{Sc} but without protease resistance occurs as an intermediate in the generation of fully proteinase-resistant PrP^{Sc} (ref. 4). No PrP 27–30 was found in normal homogenates or immunoprecipitates with protein A only (Fig. 1b) or 6H4 (not shown). 15B3 therefore seems to be a PrP^{BSE}-specific antibody, even though we immunized with recombinant bovine PrP. Injection of rbPrP into Tg20 mice overexpressing mouse PrP^5 has not produced disease for 430 days, whereas two out of four mice injected with a homogenate from the medulla of a BSE-affected cow have come down with TSE at 388 and 426 days (A.R., C.K. and B.O., unpublished results). In addition, it has been reported that recombinant PrP is not infectious[6]. Recombinant PrP is also not protease-resistant, which is a hallmark of PrP^{Sc} (C.K., unpublished observation)[7,8]. The model of Lansbury and Caughey[9], which postulates that the two isoforms of PrP are in a dynamic equilibrium, provides a possible explanation for these findings. By immunizing with large amounts of normal PrP, a small portion of the protein might, according to this hypothesis, have been in the scrapie-specific conformation when triggering the immune response. Alternatively, recombinant PrP molecules might transi-

ently associate (see below and Fig. 3b), and thereby form the prion-specific epitope when acting as an immunogen.

We further analysed the species specificity of 15B3 using mouse scrapie-infected brain homogenates (Fig. 1c) and brain homogenates from CJD type-1 patients (Fig. 1d)[10]. For comparison, the mouse brain homogenates of PrP-null as well as normal and scrapie-infected wild-type mice, and the immunoprecipitates corresponding to twice the amount of the homogenates are shown (Fig. 1c). Mouse PrP^{Sc} could be efficiently precipitated by 15B3, as indicated by the presence of PrP 27–30 after the digestion with proteinase K (Fig. 1c, lane a). When brain homogenate was treated with proteinase K before the precipitation, 15B3 was also able to precipitate PrP 27–30 (Fig. 1c, lane b), indicating that the N-terminal segment 23–90 is not critical for binding of 15B3 to PrP^{Sc}, even though precipitation of intact PrP^{Sc} appeared to be more efficient than that of PrP 27–30. Proteinase K digestion causes the formation of large aggregates (scrapie-associated fibrils) which may mask the 15B3 epitope. Surprisingly, 15B3 also specifically recognized PrP^{CJD} from sporadic CJD cases but not human PrP^C (Fig. 1d), even though the amino-acid sequence in the regions of the 15B3 epitope is not fully conserved (see below, and Fig. 2b).

The epitopes recognized by the two antibodies were determined by using a gridded array of synthetic peptides consisting of 104 13-residue peptides sequentially shifted in steps of two amino acids and covering the whole mature bovine PrP sequence. A single linear epitope (DYEDRYYRE; corresponding to positions 144–152 of human PrP[11]) was mapped for 6H4, whereas three distinct peptide sequences were found to form the 15B3 epitope (amino acids
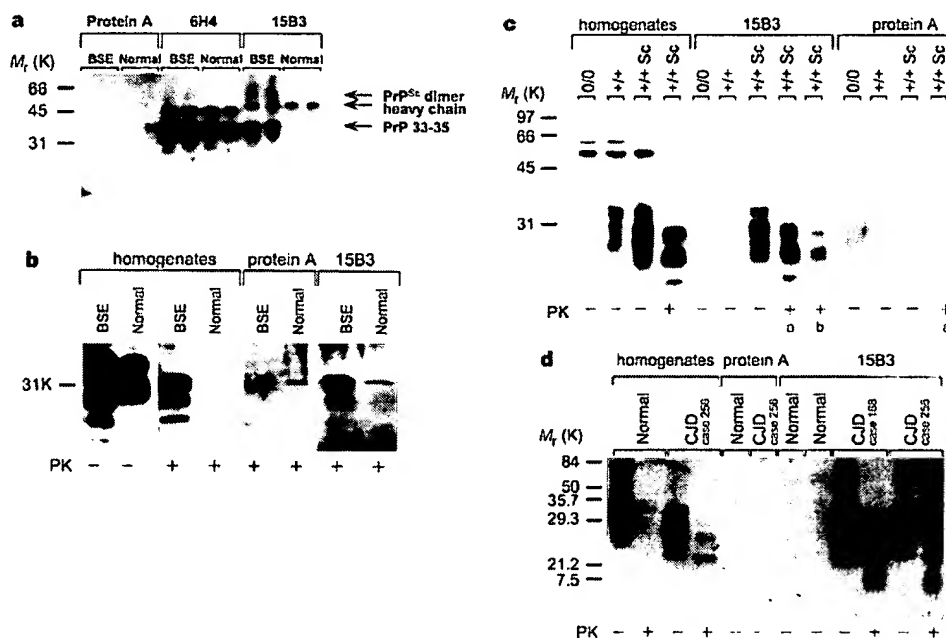

Figure 1 Immunoprecipitation of bovine, mouse and human PrP with monoclonal antibodies 15B3 and 6H4. **a**, The supernatant of a centrifuged homogenate from the medulla of two different BSE-diagnosed or two normal animals was incubated with antibodies 6H4 or 15B3. Antibodies were precipitated with protein A- (15B3) or protein G-agarose (6H4). As a control, protein A only was incubated without antibodies. Precipitates were analysed on a western blot for the presence of PrP using a polyclonal rabbit antiserum to bovine PrP and goat-anti-rabbit Ig coupled to alkaline phosphatase. Signals were developed with chemiluminescence substrates. Crossreaction of the secondary antibody with immunoprecipitated mouse immunoglobulins leads to the prominent band at about 50K. Note the 60K band characteristic for PrP^{Sc} in the 15B3 but not in the 6H4 immunoprecipitations. **b**, Proteinase K digestion of PrP^{BSE} immunoprecipitated with mA 15B3. Undigested and digested bovine brain homogenates were compared to proteinase K digested immunoprecipitates with protein A-agarose only or with 15B3. The sharp band at 31K represents a crossreactivity of the secondary antibody with proteinase K. The same immunoprecipitates and method of analysis were used as in a. **c**, Immunoprecipitation of mouse PrP^{Sc} with mAb 15B3. Homogenates from PrP-null mice (0/0) or wild-type mice (normal (+/+) or scrapie-infected (+/+Sc)) were immunoprecipitated with mAB 15B3 or protein A-agarose only and analysed by western blotting as described. Digestion with proteinase K after (a) or before (b) the immunoprecipitation is indicated. Detection of PrP was done as described. **d**, Immunoprecipitation of human PrP^{CJD} with mAb 15B3. Brain homogenates (cerebellum) from normal persons or CJD patients type 1 (ref. 10) were immunoprecipitated and analysed as described for a. Two representative examples from a total of 4 normal persons and 4 CJD cases are shown.
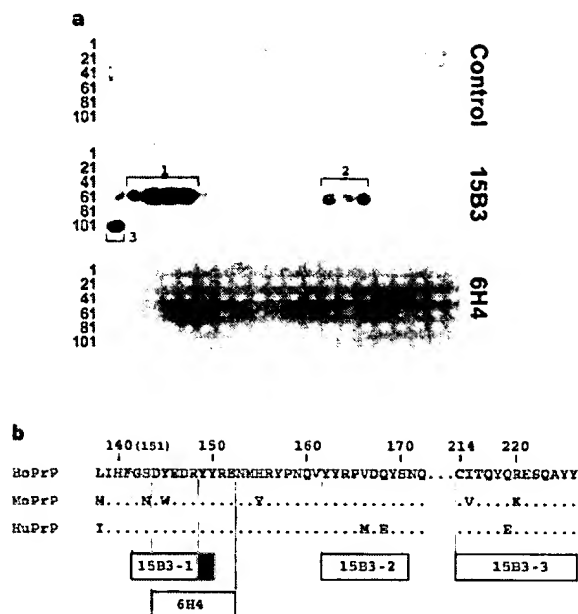
142–148, 162–170, and 214–226; Fig. 2a, b). The relative positions of these partial epitopes in the amino-acid sequence revealed an overlap of the 6H4 epitope with the first segment of the 15B3 epitope (Fig. 2b).

Mapping of the 15B3 epitope onto the NMR structure of the C-terminal domain of mouse PrP (ref. 12) reveals close proximity of the peptide segments 2 and 3, but a much larger spatial separation of the segment 1 from either of the other two components (Fig. 3a). The peptide segment 1 occupies the N-terminal half of helix 1 plus the two residues preceding it, and it is recognized by 6H4 in PrP^C as well as by 15B3 in PrP^{Sc}. This finding would be compatible with either of the two following assumptions: (1) 15B3 recognizes segment 1 of its epitope only in concert with the segments 2 and 3; (2) the polypeptide segment of helix 1 is differently folded in PrP^C and PrP^{Sc}. Component 2 of the 15B3 epitope is in the loop connecting the second β-strand to the second helix, with two thirds of it in a disordered region in the three-dimensional structure, and component 3 is located at the C-terminal end of helix 3 (refs 12, 13). The peptide segments 2 and 3 are located in the proposed binding region for 'protein X' (ref. 14), which is characterized by significant alterations of the electrostatic surface potential among different mammalian species[15]: human PrP differs from bovine and mouse PrP in the replacement of the glutamine residues 168 and 219 by glutamic acid residues, as well as by conservative substitutions at positions 166 and 215. As bovine, mouse and human PrP^{Sc} are all precipitated by 15B3 (Fig. 1a–d), this antibody probably binds to the conserved residues in this region.

A single continuous 15B3 binding site could be formed either by aggregation of two or several PrP molecules[16], or by structural rearrangement of a single PrP molecule, or by a combination thereof. Figure 3b suggests a spatial arrangement of a PrP dimer that would bring all three segments of the 15B3 epitope into spatial proximity, with minimal conformational changes of the individual molecules. It is based on the observation of a structural similarity between PrP(121–231) and haemoglobins, which allows a superposition of the helices 1, 2 and 3 of PrP^C onto the helices 1, 6 and 7 of the haemoglobin β-subunit, with a root-mean-square distance for the polypeptide backbone of 2.4 Å. Superposition of two molecules
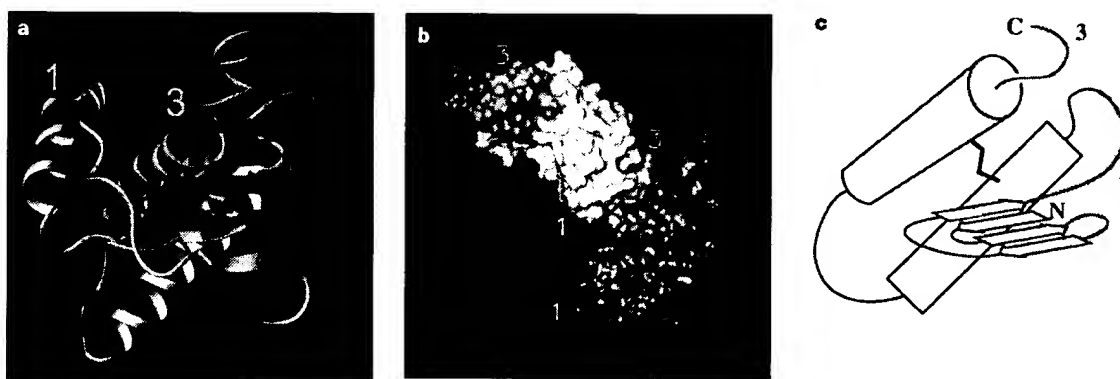
Figure 2 Determination of epitopes for mAbs 15B3 and 6H4. A gridded array of synthetic peptides corresponding to bovine PrP was incubated with 15B3, 6H4 or with secondary antibody only (peroxidase-labelled goat anti-mouse Ig; control). Bound antibody was visualized with chemiluminescence. Each spot corresponds to a 13-amino-acid peptide, which is shifted by two amino acids along the bovine PrP sequence relative to the previous peptide. Peptides were covalently attached at the C terminus to a cellulose support. A total of 104 peptides were used to cover the whole bovine PrP sequence including the six octapeptide repeat sequences[21]. **b**, Minimal sequences recognized by 15B3 or 6H4 antibodies in the array of synthetic bovine PrP peptides. The polypeptide segments of the 15B3 epitope are numbered as they occur in the amino acid sequence. The first 15B3 segment extends by two amino acids C-terminally (grey box) if spot number 62, which binds 15B3 only weakly, is excluded. The numbering of the sequence is according to human PrP[11]; the number in brackets indicates the position in the bovine PrP sequences used for the construction of the array of synthetic peptides. Differences with the human and mouse PrP sequences are indicated.

Figure 3 The epitope of the monoclonal antibody 15B3 in the three-dimensional prion protein structure. **a**, Mapping of the 15B3 epitope onto a ribbon drawing of the NMR structure of the C-terminal domain PrP(121–231) of mouse PrP^C (refs 12, 26). The three segments of the 15B3 epitope are coloured yellow (1), violet (2) and cyan (3) in the order in which they occur in the amino acid sequence (Fig. 2b). The residual parts of the molecule and the single disulphide bridge are grey. Regular secondary structures are indicated by ribbons for helices and arrows for β-strands. Drawings in **a** and **b** were prepared with MOLMOL[27]. **b**, Surface representation of two PrP(121–231) molecules after superposition onto two β-subunits of the crystal lattice of sickle cell haemoglobin[17] (Protein Data Bank entry 1HBS). The segments of the 15B3 epitope are numbered and coloured as in **a**. The superposition included the backbone atoms of residues 145–154, 179–189 and 201–217 of the helices 1, 2 and 3 of PrP(121–231) and of residues 5–14, 106–116 and 125–141 of the helices 1, 6 and 7 of haemoglobin S (r.m.s.d. = 2.4 Å). **c**, Hypothetical fold of the prion protein that would bring all three components of the 15B3 epitope into spatial proximity. The two cylinders represent the disulphide-linked helices 2 and 3 in the orientation of **a**. Helix 1 and the β-sheet have been replaced by four β-strands that form a greek key motif. The chain termini are labelled N and C, and the segments of the 15B3 epitope are numbered as in **a**.

of PrP(121–231) onto two adjacent β-chains in the crystal lattice of haemoglobin S[17] (PDB entry 1HBS) brings the peptide segment 1 of one PrP molecule near to the segments 2 and 3 of the other molecule (Fig. 3b). This superposition aligns residue 6 of the β-chains of sickle cell haemoglobin with Trp at position 145 of the mouse prion protein, which is located in the middle of the epitope segment 1 and is fully exposed to solvent. Mutation of Glu 6 to valine is responsible for the formation of haemoglobin aggregates in sickle cell anaemia.

Intramolecular structural rearrangement bringing all three segments of the 15B3 epitope into close spatial proximity might involve the first helix and lead to an extension of the existing β-sheet[13]. In Fig. 3c, the resulting β-structure is assumed to consist of four strands aligned to form a greek-key motif. Other PrP^{Sc} models that would also lead to close approach of the three segments of 15B3 epitope have been described[18].

The identification of an antibody that binds selectively to PrP^{Sc} from various species provides a new means to identify PrP^{Sc} directly without using proteinase K digestion as a criterion. It will be interesting to see whether 15B3 will be able to neutralize infectivity and thus be a potential therapeutic reagent. The low level of PrP^{Sc} in peripheral tissues has made it difficult to use it as a marker for prion diseases[19]. Affinity selection of PrP^{Sc} with 15B3 will allow enrichment of the abnormal isoform of PrP and thus lower the detection limit for PrP^{Sc}, so a prion test for living humans or animals is conceivable. The mapping and three-dimensional modelling of the 15B3 epitopes has provided a view of a prion-disease-specific epitope and may represent a starting point for the production of further diagnostic or therapeutic tools for TSEs. □

Methods

Materials. BSE material was from naturally occurring Swiss cases of BSE, CJD brain material from patients suffering from CJD type 1 (ref. 10), which had been diagnosed using histopathology and immunohistochemistry for PrP. For mouse scrapie material, CD-1 mice were experimentally infected with the RML strain[20].

Preparation of recombinant bovine PrP. The bovine PrP open reading frame was amplified by PCR from genomic DNA using the primers 5'-GGGAATTC-CATATGAAGAAGCGACCAAAACCTG and 5'-CGGGATCCTATTAACTTG-CCCCTCGTTGGTA. The resulting PCR product was cloned into pET11a (Novagen) using the NdeI and the BamHI restriction sites. The resulting plasmid (pbPrP3) was transfected into E. coli BL21(DE3). Bacteria were grown to $OD_{600} = 0.8$ then induced with 1 mM IPTG and further grown at 30 °C for 3 h. rbPrP corresponding to the mature form of bovine PrP containing six octarepeats[21] was purified from inclusion bodies after solubilization in 8 M urea, 10 mM MOPS/NaOH, pH 7.0 (UM-buffer), on a CM sepharose column (Pharmacia; UM, 0–0.5 M NaCl gradient) and reverse-phase HPLC (Vydac C$_4$ column, 0.1% trifluoroacetic acid, 0–60% acetonitrile gradient; C.K. and B.O., unpublished results). Resulting fractions contained either oxidized (elution time, 29 min) or reduced PrP (elution time, 34 min). Usually, CM-Sepharose fractions were oxidized with 1 μM CuSO$_4$ for 1 h before purification by reverse-phase HPLC. Purified rbPRP was analysed by mass spectrometry, indicating a protein of the expected mass in which the N-terminal methionine was uncleaved.

Immunization of PrP-null mice. 100 μg recombinant bovine PrP in Freund's complete adjuvant was injected into PrP null mice (mixed background 129/Sv and C57BL/6J[22]) subcutaneously, and 21 and 42 d later with the same amount of antigen in Freund's incomplete adjuvant. Mice were boosted intraperitoneally (day 48) and intravenously (day 49) with recombinant PrP dissolved in PBS. At day 50, mice were decapitated and splenocytes fused to myeloma cells as described[23]. Supernatants of the resulting hybridoma cell lines were screened both by ELISA with recombinant bovine PrP as antigen and by ELIFA[24] using native, protease-digested brain homogenate of BSE-diseased cattle. Positive hybridoma cells were subcloned three times.

Characterization of antibodies. Supernatants of selected hybridomas were used to probe bovine PrP in brain homogenates or recombinant PrP on western blots. To determine the epitopes, antibodies were incubated with a gridded array of peptides comprising 104 polypeptides of 13 amino acids, shifted by two

amino acids and covering the entire mature bovine PrP sequence containing six octapeptide repeats[21]. The peptides were covalently attached at their C termini to a cellulose support as individual spots (Jerini Biotools, Berlin). Bound antibody was detected with goat anti-mouse immunoglobulin coupled to horseradish peroxidase and chemiluminescence. Signals were recorded on Hyperfilm ECL (Amersham). For immunoprecipitation, 200 μl 1% brain homogenates (precleared by centrifugation at 13,000g for 15 min) were incubated for 2 h at room temperature with 200 μl 0.25 mg ml^{-1} antibody-containing serum-free medium; after incubation with an additional 50 μl protein A- or protein G-coupled agarose (for 15B3 and 6H4, respectively; Boehringer Mannheim) for 2 h at room temperature, agarose beads were centrifuged at 13,000g for 3 min and the pellet washed according to the manufacturer. Proteinase K (PK) digestions of immunoprecipitates were done with 20 μg ml^{-1} PK (Sigma) for 30 min at 37 °C. Pellets were then boiled in SDS-sample buffer for analysis on western blots. Immunoprecipitated PrP was detected with polyclonal antibodies raised against bovine recombinant PrP in rabbits (R 26) followed by incubation with a goat anti-rabbit immunoglobulin coupled to peroxidase or a goat anti-rabbit IgG coupled to alkaline phosphatase. Bound enzymatic activity was visualized with chemiluminescent substrates (ECL, Amersham, or CSPD, Tropix, respectively).

1. Pan, K. M. et al. Conversion of alpha-helices into beta-sheets features in the formation of the scrapie prion proteins. Proc. Natl Acad. Sci. USA 90, 10962–10966 (1993).
2. McKinley, M. P., Bolton, D. C. & Prusiner, S. B. A protease-resistant protein is a structural component of the scrapie prion. Cell 35, 57–62 (1983).
3. Oesch, B. et al. A cellular gene encodes scrapie PrP 27–30 protein. Cell 40, 735–746 (1985).
4. Daude, N., Lehmann, S. & Harris, D. A. Identification of intermediate steps in the conversion of a mutant prion protein to a scrapie-like form in cultured cells. J. Biol. Chem. 272, 11604–11612 (1997).
5. Fischer, M. et al. Prion protein (PrP) with amino-proximal deletions restoring susceptibility of PrP knockout mice to scrapie. EMBO J. 15, 1255–1264 (1996).
6. Mehlhorn, I. et al. High-level expression and characterization of a purified 142-residue polypeptide of the prion protein. Biochemistry 35, 5528–5537 (1996).
7. Weiss, S., Rieger, R., Edenhofer, F., Fisch, E. & Winnacker, E. L. Recombinant prion protein rPrP27-30 from Syrian golden hamster reveals proteinase K sensitivity. Biochem. Biophys. Res. Commun. 219, 173–179 (1996).
8. Kaneko, K. et al. Molecular properties of complexes formed between the prion protein and synthetic peptides. J. Mol. Biol. 270, 574–586 (1997).
9. Lansbury, P. T. & Caughey, B. The chemistry of scrapie infection: implications of the 'ice 9' metaphor. Chem. Biol. 2, 1–5 (1995).
10. Parchi, P. et al. Molecular basis of phenotypic variability in sporadic Creutzfeldt–Jakob disease. Ann. Neurol. 39, 767–778 (1996).
11. Schätzl, H. M., Da Costa, M., Taylor, L., Cohen, F. E. & Prusiner, S. B. Prion protein gene variation among primates. J. Mol. Biol. 245, 362–374 (1995).
12. Riek, R. et al. NMR structure of the mouse prion protein domain PrP(121–231). Nature 382, 180–182 (1996).
13. Glockshuber, R. et al. Three-dimensional NMR structure of a self-folding domain of the prion protein PrP (121–231). Trends Biochem. Sci. 22, 241–242 (1997).
14. Telling, G. C. et al. Prion propagation in mice expressing human and chimeric PrP transgenes implicates the interaction of cellular PrP with another protein. Cell 83, 79–900 (1995).
15. Billeter, M. et al. Prion protein NMR structure and species barrier for prion diseases. Proc. Natl Acad. Sci. USA 84, 7281–7285 (1997).
16. Warwicker, J. & Gane, P. J. A model for prion protein dimersization based on alpha-helical packing. Biochem. Biophys. Res. Commun. 226, 777–782 (1996).
17. Padian, E. A. & Love, W. E. Refined crystal structure of deoxyhemoglobin S. II. Molecular interactions in the crystal. J. Biol. Chem. 260, 8280–8291 (1985).
18. Huang, Z., Prusiner, S. B. & Cohen, F. E. Scrapie prions: a three-dimensional model of an infectious fragment. Fold. Design 1, 13–19 (1996).
19. Kitamoto, T., Mohri, S. & Tateishi, J. Organ distribution of proteinase-resistant prion protein in humans and mice with Creutzfeldt–Jakob disease. J. Gen. Virol. 70, 3371–3379 (1989).
20. Chandler, R. L. Encephalopathy in mice produced by inoculation with scrapie brain material. Lancet i, 1378–1379 (1961).
21. Goldmann, W., Hunter, N., Martin, T., Dawson, M. & Hope, J. Different forms of the bovine PrP gene have five or six copies of a short, G-C-rich element within the protein-coding exon. J. Gen. Virol. 72, 201–204 (1991).
22. Bueler, H. et al. Normal development and behaviour of mice lacking the neuronal cell-surface PrP protein. Nature 356, 577–582 (1992).
23. Kennett, R. H. Monoclonal Antibodies. Hybridomas: A New Dimension in Biological Analysis (eds Kennett, R. H., McKearn, T. J. & Bechtol, K. B.) 365–367 (Plenum, New York, 1980).
24. Oesch, B., Jensen, M., Nilsson, P. & Fogh, J. Properties of the scrapie prion protein: quantitative analysis of protease resistance. Biochemistry 33, 5926–5931 (1994).
25. Priola, S. A., Caughey, B., Wehrly, K. & Chesebro, B. A 60-kDa prion protein (PrP) with properties of both the normal and scrapie-associated forms of PrP. J. Biol. Chem. 270, 3299–3305 (1995).
26. Riek, R., Hornemann, S., Wider, G., Glockshuber, R. & Wuthrich, K. NMR characterization of the full-length recombinant murine prion protein, mPrP(23–231). FEBS Lett. 413, 282–288 (1997).
27. Koradi, R., Billeter, M. & Wuthrich, K. MOLMOL: a program for display and analysis of macromolecular structures. J. Mol. Graph. 14, 51–55 (1996).

Correspondence and requests for materials should be addressed to C.K. (e-mail: ckorth@hifo.unizh.ch) or B.O. (e-mail: oesch@hifo.unizh.ch).

nature
medicine

A prion protein epitope selective for the pathologically misfolded conformation

Eustache Paramithiotis[1], Marc Pinard[1], Trebor Lawton[2], Sylvie LaBoissiere[1], Valerie L Leathers[2], Wen-Quan Zou[6], Lisa A Estey[2], Julie Lamontagne[1], Marty T Lehto[6], Leslie H Kondejewski[1], Gregory P Francoeur[2,8], Maria Papadopoulos[1], Ashkan Haghighat[1], Stephen J Spatz[2,9], Mark Head[3], Robert Will[3], James Ironside[3], Katherine O'Rourke[4], Quentin Tonelli[2], Harry C Ledebur[1], Avi Chakrabartty[5] & Neil R Cashman[1,5,6,7]

Conformational conversion of proteins in disease is likely to be accompanied by molecular surface exposure of previously sequestered amino-acid side chains. We found that induction of β-sheet structures in recombinant prion proteins is associated with increased solvent accessibility of tyrosine. Antibodies directed against the prion protein repeat motif, tyrosine-tyrosine-arginine, recognize the pathological isoform of the prion protein but not the normal cellular isoform, as assessed by immunoprecipitation, plate capture immunoassay and flow cytometry. Antibody binding to the pathological epitope is saturable and specific, and can be created in vitro by partial denaturation of normal brain prion protein. Conformation-selective exposure of Tyr-Tyr-Arg provides a probe for the distribution and structure of pathologically misfolded prion protein, and may lead to new diagnostics and therapeutics for prion diseases.

The prion diseases are a group of neurodegenerative disorders characterized by neuronal cell loss, spongiform change, gliosis and deposition of abnormal amyloid protein[1-3]. Animal prion diseases include scrapie in sheep and goats, bovine spongiform encephalopathy (BSE) in cattle, chronic wasting disease in deer and elk, transmissible mink encephalopathy, and feline spongiform encephalopathy in domestic and exotic cats. In humans, recognized prion diseases include kuru, classical Creutzfeldt-Jakob disease (CJD), Gerstmann-Sträussler-Scheinker syndrome (GSS), fatal familial insomnia and variant Creutzfeldt-Jakob disease (variant CJD). Of particular recent concern is variant CJD, presumably resulting from oral inoculation of BSE prions. Currently, cases of this emergent prion disease have been identified in the United Kingdom, France, the Republic of Ireland, Hong Kong, Italy, the United States and Canada[2,3]. There is no authoritative consensus on the ultimate extent of the primary variant CJD epidemic, nor to the risk of secondary human-to-human transmission by iatrogenic routes.

The 'protein-only' hypothesis contends that prion infectivity resides in pathologically misfolded prion protein (designated PrP^{Sc}, PrP^{BSE}, or PrP^{CJD}, depending on the species of origin; PrP^{Sc} is used here to denote disease-associated PrP), which can 'recruit' cellular prion protein (PrP^C) by a template-directed process[1]. PrP^{Sc} generally possesses partial protease resistance and high β-sheet content, unlike the protease-sensitive, α-helix-rich PrP^C (refs. 4–6). As a distinct structural isoform of PrP, one would anticipate that PrP^{Sc} should

possess unique conformational epitopes. A 'shotgun' immunization of PrP-null mice with recombinant bovine PrP has yielded a single putative IgM monoclonal antibody to PrP^{Sc} (ref. 7), the specificity of which has not been confirmed outside of the reporting laboratory (refs. 8,9 and data not shown). We now report that antibody access to the PrP repeat motif Tyr-Tyr-Arg defines a PrP^{Sc}-selective epitope.

RESULTS

PrP tyrosine exposure is dependent on conformation

PrP^{Sc} is poorly soluble and tends to aggregate under physiological conditions[4-6], properties often associated with molecular surface exposure of hydrophobic amino-acid side chains. We hypothesized that side chains not normally exposed to solvent might participate in the formation of unique immunological epitopes for selective antibody recognition of PrP^{Sc}. Low-pH treatment of recombinant PrP induces increased β-sheet content and promotes aggregation, perhaps modeling aspects of the conformational conversion of PrP^C to PrP^{Sc} in disease (refs. 10–12 and data not shown). We now report that low-pH treatment of full-length recombinant mouse PrP is accompanied by increased solvent exposure of tyrosine side chains, as indicated by increased tyrosine-specific fluorescence (Fig. 1a) and enhanced access to the collisional quenching agent acrylamide[13] (Fig. 1b). In contrast, tryptophan-specific fluorescence was unchanged at low pH (Fig. 1a), with no observable change in acrylamide fluorescence quenching (data not shown). As virtually all tyrosine residues reside in the C-ter-

[1]Caprion Pharmaceuticals Inc., 7150 Alexander-Fleming, St-Laurent, Quebec H4S 2C8, Canada. [2]IDEXX Laboratories Inc., 1 IDEXX Drive, Westbrook, Maine 04092, USA. [3]The National Creutzfeldt-Jakob Disease Surveillance Unit, Western General Hospital, Crewe Road, Edinburgh EH4 2XU, UK. [4]USDA-ARS-ADRU, 3003 ADBF, Washington State University, Pullman, Washington 99164-6630, USA. [5]Department of Medical Biophysics, University of Toronto, Ontario Cancer Institute, 610 University Avenue, Toronto, Ontario M5G 2M9, Canada. [6]Centre for Research in Neurodegenerative Diseases, 6 Queen's Park Crescent West, University of Toronto, Toronto, Ontario M5S 3H2, Canada. [7]Sunnybrook & Women's College Health Sciences Centre, University of Toronto, 2075 Bayview Avenue, Toronto, Ontario M4N 3M5, Canada. [8]Deceased. [9]Present address: Vertex Inc., 130 Waverly Street, Cambridge, Massachusetts 02139-4242, USA. Correspondence should be addressed to N.R.C. (neil.cashman@utoronto.ca).
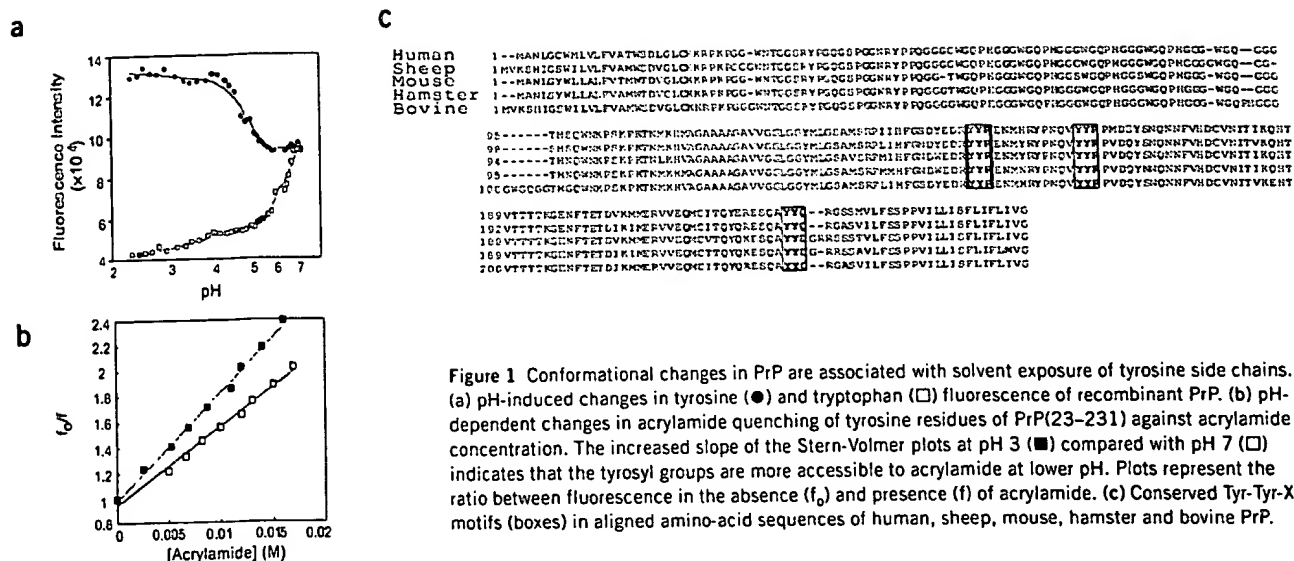
a

b

c

Figure 1 Conformational changes in PrP are associated with solvent exposure of tyrosine side chains. (a) pH-induced changes in tyrosine (●) and tryptophan (□) fluorescence of recombinant PrP. (b) pH-dependent changes in acrylamide quenching of tyrosine residues of PrP(23–231) against acrylamide concentration. The increased slope of the Stern-Volmer plots at pH 3 (■) compared with pH 7 (□) indicates that the tyrosyl groups are more accessible to acrylamide at lower pH. Plots represent the ratio between fluorescence in the absence (f_0) and presence (f) of acrylamide. (c) Conserved Tyr-Tyr-X motifs (boxes) in aligned amino-acid sequences of human, sheep, mouse, hamster and bovine PrP.

minal two-thirds of PrP, changes in tyrosine solvent access are probably indicative of conformational changes in this 'structured domain'[14–16], which also contributes to the infectious, protease-resistant fragment of PrP^{Sc} (refs. 4–6).

Tyr-Tyr-Arg antibodies selectively recognize PrP^{Sc}

The majority of tyrosine residues in the structured domain of PrP appear in pairs conserved across mouse, hamster, sheep, bovine and human PrP (Fig. 1c). Two tyrosine pairs, located in α-helix 1 and β-strand 2, are found in conjunction with a C-terminal arginine (human sequence residues 149–151 and 162–164, respectively), whereas a tyrosine pair at the C terminus of helix 3 (residues 225–227) is flanked by a C-terminal aspartate in mouse and hamster or a glutamine in sheep, bovine and human PrP. We reasoned that the increased solvent exposure of tyrosyl side chains in β-sheet-rich recombinant PrP might involve at least one such bi-tyrosine motif. Furthermore, if recombinant β-sheet-rich models some structural features of PrP^{Sc} (refs. 10–12), antibody access to one or several Tyr-Tyr-X motifs may provide a PrP^{Sc}-selective conformational epitope.

To test this hypothesis, rabbits were immunized with Tyr-Tyr-Arg-NH$_2$ peptides coupled through an N-terminal cysteine residue to keyhole limpet hemocyanin (KLH). Purified rabbit IgG fractions were conjugated to magnetic beads and used in immunoprecipitation experiments with normal and prion-infected brain homogenates (see Supplementary Methods online). This bead-conjugated antibody (designated C2) specifically immunoprecipitated PrP^{Sc} from ME7 scrapie-infected mouse brain homogenates (Fig. 2a, lanes 11 and 12; Table 1) but not PrP^C from uninfected brains (Fig. 2a, lanes 9 and 10). Additionally, the C2 polyclonal antibody immunoprecipitated the protease-resistant core of PrP^{Sc} (PrP(27–30)) from protease K–treated mouse scrapie brain homogenates (Fig. 2a, lane 12), indicating that its reactivity was not directed against the protease-sensitive domain of PrP^{Sc} (residues 23 to ~90) or against a protease-sensitive coprecipitated protein. As controls, magnetic beads coupled with monoclonal antibody 6H4, which recognizes an epitope present on both PrP^C and PrP^{Sc} (ref. 7), immunoprecipitated PrP from both normal and prion-infected brain (Fig. 2a, lanes 1–4), whereas beads coupled to BSA (Fig. 2a, lanes 5–8) or preimmune sera (Table 1) precipitated neither PrP iso-

form. Similar results were obtained with goat polyclonal IgG against KLH-Cys-Tyr-Tyr-Arg (Table 1).

Table 1 Species reactivity of PrP^{Sc}-selective Tyr-Tyr-Arg antibodies

	Mouse	Hamster	Sheep	Bovine	Human
Polyclonals					
Rabbit C2	++	+	ND	ND	ND
Goat p165	++	+	ND	ND	ND
Monoclonals					
1A12	++	++	++	+	+[a]
17D10	++	++	+	+	++
17D4	++	++	+	+	++
16A18	++	++	+	+	++[a]
20A13	+	+	+	+	ND
1A7	++	+	–	+	ND
3A2	+	++	–	+	ND
9A4	++	++	++	++	+
12A5	++	++	–	+	ND
12B1	++	++	++	++	++[b]
Recombinants					
16A18	++	ND	ND	ND	ND
20A13	++	ND	ND	ND	ND
1A7	+	ND	ND	ND	ND
9A4	++	ND	ND	ND	ND
12A5	++	ND	ND	ND	ND
Control antibodies					
Rabbit pre	–	–	ND	ND	ND
Goat pre	–	–	ND	ND	ND
4E4 IgM	–	–	–	–	–
10D4 IgM	–	–	–	–	–
115 IgM	–	–	–	–	–

Tyr-Tyr-Arg antibodies recognize PrP^{Sc} from prion-infected brains of multiple species. Reactivity (graded –, + or ++) was compiled from at least three brain immunoprecipitations. ND, not determined; pre, pre-immune sera. We used mouse prion strains ME7 and 139A, hamster strain 263K and human prion disease strains variant CJD, classical sporadic CJD and GSS. [a]CJD and GSS only. [b]Variant CJD only.

We next generated Tyr-Tyr-Arg mono-clonal antibodies by immunizing BALB/c mice with KLH conjugated to the peptide CYYRRYYRYY (this peptide sequence was chosen because one PrP bi-tyrosine motif is flanked by arginine at both N and C termini). Sixty monoclonal antibodies were selected by ELISA screening against the Tyr-Tyr-Arg antigen coupled to a backbone comprising branched lysines (four-branch multiple antigen peptide; 4-MAP). Ten monoclonal antibodies binding 4-MAP-Tyr-Tyr-Arg, but not control 4-MAP-Ala-Ala-Ala, were tested for PrP^{Sc}-specific recognition by immunoprecipitation as described above. All ten monoclonal antibodies displayed PrP^{Sc}-specific immunoprecipitation from scrapie-infected ME7 and 139A mouse brain or 263K infected hamster brain, and from naturally prion-infected sheep and cattle (Table 1). Some monoclonal antibodies preferentially recognized PrP^{Sc} from a subset of these species, suggesting that the monoclonal antibodies did not recognize identical epitopes, a finding supported by peptide competition experiments (see below). Immuno-precipitation studies performed with two monoclonal antibodies (1A12 and 17D10) are shown (Fig. 2b). Magnetic beads coupled to the positive control monoclonal antibody 6H4 immuno-precipitated PrP from both normal and prion-infected tissues, whereas beads coupled to three isotype-control monoclonal antibodies immunoprecipitated neither PrP isoform (Fig. 2b and Table 1). In addition, monoclonal antibodies to Tyr-Tyr-Arg selectively immunoprecipitated PrP^{Sc} from prion-infected human brain homogenates (two classical sporadic CJD, one GSS, and three variant CJD) but did not immunoprecipitate PrP from 12 brains of other neurological diseases (Fig. 2c,d, Table 1 and data not shown). Direct efficiency comparison of the sensitivity of protease K digestion and T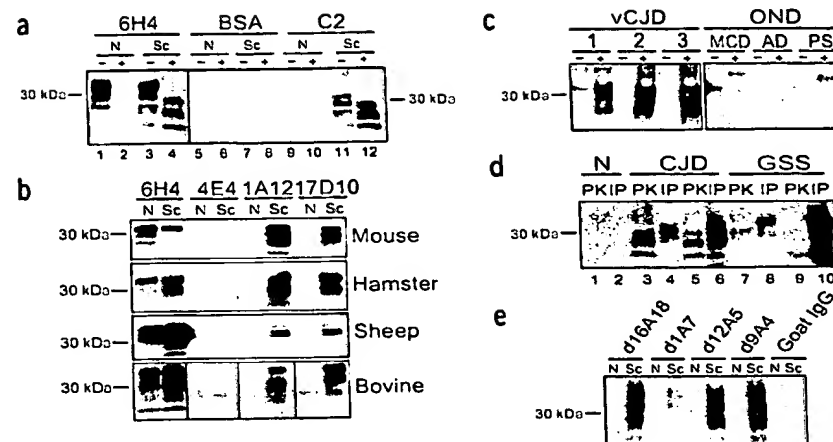yr-Tyr-Arg monoclonal antibody immunoprecipitation showed comparable signal in most species and brain regions (Fig. 2a,d) but revealed that selected prion disease brains contain immunoprecipitatable PrP, which is poorly resistant to protease K (Fig. 2d and data not shown).

Although PrP^{Sc}-specific polyclonal IgG antibodies to Tyr-Tyr-Arg have been successfully raised in rabbits (Fig. 2a) and goats (data not shown), all mouse monoclonal antibodies to Tyr-Tyr-Arg produced to date have been IgMs, even at the screening stage. In order to exclude the possibility that PrP^{Sc} recognition is a low-affinity interaction dependent on the high avidity conferred by ten IgM antigen-binding sites, we constructed and expressed chimeric IgG monoclonal anti-
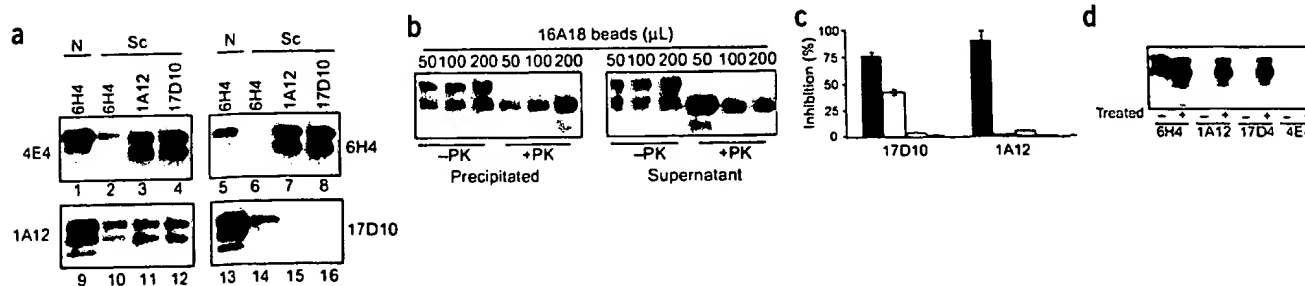

Figure 2 Tyr-Tyr-Arg antibodies selectively recognize PrP^{Sc}. (a) Rabbit polyclonal antibody (C2) selectively immunoprecipitates PrP^{Sc} and PrP(27–30) but not PrP^C. C2-conjugated magnetic beads were incubated with normal (N) or scrapie-infected (Sc) mouse brain homogenate with (+) or without (–) proteinase K (PK) treatment. (b) Monoclonal antibodies 1A12 and 17D10 selectively immunoprecipitate PrP^{Sc} from experimentally and naturally infected prion disease brain, but not PrP^C from uninfected brain. 4E4, isotype-control monoclonal antibody. (c) 17D10 immunoprecipitates PrP^{Sc} from variant CJD (vCJD)-infected brain (1, 2, 3) but not PrP^C from brains with other neurological disease (OND; MCL, multifocal calcifying leucoencephalopathy; AD, Alzheimer disease; PS, paraneoplastic syndrome) +, 17D10; –, 4E4 immunoprecipitations. (d) Efficiency comparison of PK resistance and Tyr-Tyr-Arg immunoprecipitation (monoclonal antibody 16A18) from equivalent samples of frontal (1–4, 7, 8) and cerebellar (5, 6, 9, 10) regions of a CJD and a GSS brain. (e) Chimeric dog-mouse PrP^{Sc}-specific IgG selectively precipitates PrP^{Sc}, but not PrP^C, from scrapie-infected mouse brain homogenate. Immunoprecipitated PrP was detected by immunoblotting with 6H4 (a,b,e) or 3F4 (c,d).

Figure 3 Characterization of PrP^{Sc}-selective antibodies. (a) PrP^{Sc}-selective antibodies and 6H4 recognize different sites on PrP^{Sc}. Normal (N) or scrapie-infected (Sc) hamster brain homogenates were incubated with unconjugated control IgM 4E4 (lanes 1–4), 6H4 (lanes 5–8), 1A12 (lanes 9–12) or 17D10 (lanes 13–16), followed by immunoprecipitation with magnetic bead-conjugated 6H4 (lanes 1, 2, 5, 6, 9, 10, 13 and 14), 1A12 (lanes 3, 7, 11 and 15), or 17D10 (lanes 4, 8, 12 and 16). (b) Saturability of Tyr-Tyr-Arg monoclonal antibody binding. A fixed quantity of 263K scrapie brain homogenate was probed with a titration of 16A18 monoclonal antibody beads followed by PK digestion. PrP(27–30) signal is proportional (immunoprecipitates directly, supernatants indirectly) to bead quantity. (c) 17D10 and 1A12 epitope characterization. ELISA data are presented as percent inhibition of binding compared to binding without peptide (■, 4-MAP YYR; □, 4-MAP YAR; ▨, 4-MAP YYA; ■, 4-MAP AAA). Shown are means ± s.d. ($n = 3$). (d) Monoclonal antibodies 1A12 and 17D10 selectively immunoprecipitate partially denatured human brain PrP. Lanes 2, 4, 6, 8: acidic pH- and guanidine HCl-treated brain samples; lanes 1, 3, 5, 7: mock-treated samples. Immunoprecipitated PrP was detected by immunoblotting with 6H4 (a–c) or 3F4 (d).
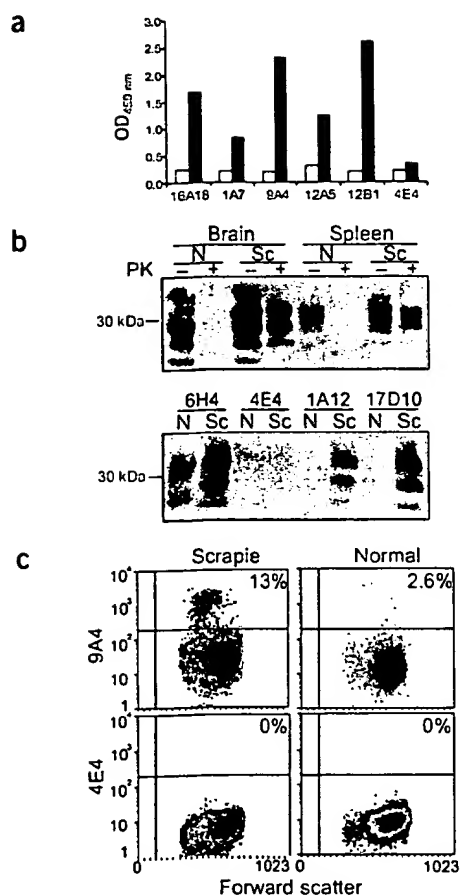
3

Figure 4 Tyr-Tyr-Arg antibodies detect PrP^{Sc} in diagnostic platforms and tissues. (a) Mouse PrP^{Sc} detected in a 96-well capture format using monoclonal antibody–conjugated beads (Tyr-Tyr-Arg monoclonal antibodies 16A18, 1A7, 9A4, 12A5, 12B1; isotype-control monoclonal antibody 4E4) and an isoform-nondiscriminating rabbit polyclonal antibody to PrP N terminus (■, scrapie; □, control). Results displayed as absorbance (OD) at 450 nm. (b) Tyr-Tyr-Arg antibodies recognize low concentrations of PrP^{Sc} in ME7-infected mouse spleen. Top, normal (N) and scrapie-infected (Sc) mouse brain and spleen homogenates were mock- (–) or protease K (PK)- digested (+) and PrP isoforms were revealed by 6H4 immunoblot. Bottom, Tyr-Tyr-Arg monoclonal antibodies 1A12 and 17D10 selectively precipitate PrP^{Sc} from scrapie-infected mouse spleen. (c) Tyr-Tyr-Arg monoclonal antibody 9A4 recognizes a population of dendritic cells from scrapie-infected sheep lymph nodes. CD58$^+$CD45RO$^-$ retropharyngeal lymph node cells from scrapie-infected and normal sheep stained with 9A4 or control monoclonal antibody 4E4.

bodies from recombinant light- and heavy-chain variable regions of five different Tyr-Tyr-Arg monoclonal antibodies in a dog IgG frame-work[17]. All five recombinant bivalent IgG antibodies retained selective immunoprecipitation activity against PrP^{Sc} (Fig. 2e and Table 1), con-sistent with a relatively high-affinity recognition of PrP^{Sc} by the native IgM monoclonal antibodies. Tyr repeats have been reported to define a dominant B-cell epitope[18], suggesting that the highly skewed IgM monoclonal antibody frequency we observed may be the result of a specific mouse immune response to Tyr-Tyr-Arg antigens.

The PrP^{Sc} Tyr-Tyr-Arg epitope is saturable and specific
We carried out antibody competition experiments to test the immunological authenticity of the PrP^{Sc}-selective Tyr-Tyr-Arg epi-tope (Fig. 3a). Scrapie-infected hamster brain homogenates were incubated overnight with soluble Tyr-Tyr-Arg monoclonal antibodies 1A12 and 17D10, or the nondistinguishing PrP antibody 6H4, or the control antibody 4E4. These homogenates were then subjected to immunoprecipitation with the same series of antibodies covalently coupled to magnetic beads. Whereas pretreatment with soluble 1A12 or 17D10 inhibited the immunoprecipitation of PrP^{Sc} by either bead-conjugated Tyr-Tyr-Arg monoclonal antibody, neither soluble 6H4 nor 4E4 monoclonal antibodies blocked PrP^{Sc} immunoprecipitation by 1A12 and 17D10. Similarly, 1A12 and 17D10 did not block the immunoprecipitation of PrP^C or PrP^{Sc} with 6H4, despite the overlap of the reported 6H4 epitope and a Tyr-Tyr-Arg motif in helix 1 (ref. 7). The saturability of the PrP^{Sc}–monoclonal antibody interac-tion was also tested by titration of 263K hamster scrapie brain

homogenate with Tyr-Tyr-Arg 16A18-conjugated beads (Fig. 3b), showing that bead quantity is proportional to PrP^{Sc} and PrP(27–30) content of immunoprecipitates and supernatants. These data are con-sistent with specific and saturable immune recognition of a discrete PrP^{Sc} epitope by antibodies to Tyr-Tyr-Arg.

To further characterize the Tyr-Tyr-Arg epitope, the fine specifici-ties of 1A12 and 17D10 were determined in a peptide competition ELISA system (Fig. 3c). As expected, the two Tyr-Tyr-Arg mono-clonal antibodies bound to plate-immobilized 4-MAP-Tyr-Tyr-Arg, but the isotype-control monoclonal antibody 4E4 and the isoform-nonspecific monoclonal antibody 6H4 did not (data not shown). Plate binding of 1A12 and 17D10 was efficiently inhibited by soluble 4-MAP-Tyr-Tyr-Arg, but not by 4-MAP-Ala-Ala-Ala. Tyr-Tyr-Ala conjugate did not compete for binding of 1A12 or 17D10, whereas Tyr-Ala-Arg conjugate partially competed for the binding of 17D10, but not 1A12. These data suggest that 1A12 and 17D10 possess over-lapping, but not identical, specificities in which all three amino-acid side chains participate in epitope recognition, although access to the terminal tyrosine and arginine residues may be more important than the central tyrosine.

Our data indicate that the PrP^{Sc}-specific Tyr-Tyr-Arg epitope must be cryptic in PrP^C, but exposed to antibody binding in PrP^{Sc}. Efforts to immunoprecipitate β-sheet-rich recombinant mouse PrP treated at low pH (Fig. 1a,b) revealed that this preparation bound non-specifically to all tested antibodies, including isotype-control mono-clonal antibodies (data not shown). However, PrP^C in normal human and mouse brain homogenates treated under identical con-ditions[19] acquires the Tyr-Tyr-Arg epitope (Fig. 3d and data not shown), suggesting that the tripeptide epitope is exposed when PrP is partially denatured in the context of native post-translational modi-fications (including two N-linked glycans and a glycosyl-phos-phatidylinositol anchor).

PrP^{Sc} Tyr-Tyr-Arg reactivity is platform-independent
Using a 96-well sandwich ELISA system, we observed PrP^{Sc} detection sensitivity with Tyr-Tyr-Arg monoclonal antibodies for capture, and a pan-PrP N-terminus polyclonal antibody for detection (Fig. 4a). In these experiments, scrapie-to-normal ratios ranged up to 25-fold for the panel of monoclonal antibodies tested, using a 1,000-fold final dilution of mouse ME7 scrapie brain. These data suggest that Tyr-Tyr-Arg antibodies may be useful in a robust high-throughput immunodetection system targeted against native PrP^{Sc}.

Several important natural prion diseases (such as scrapie and vari-ant CJD) are accompanied by agent accumulation in biopsy-accessi-

ble peripheral lymphoid tissues. In mouse spleen, however, prion titers are at least 3–4 logs lower than those in brain[20,21], and PrP(27–30) load in moribund animals is estimated to be at least 1–2 logs less than that of brain[21,22]. Despite low levels of PrP^{Sc} in spleen compared with brain (Fig. 4b, upper panel), Tyr-Tyr-Arg monoclonal antibodies 17D10 and 1A12 immunoprecipitated PrP^{Sc} from this tissue, but not PrP^C (Fig. 4b, bottom panel). These data indicate that the sensitivity of the Tyr-Tyr-Arg monoclonal antibodies is sufficient to maintain PrP isoform specificity even in the presence of high concentrations of heterologous proteins.

In diseases accompanied by lymphoid replication of prions, PrP^{Sc} preferentially accumulates in follicular dendritic cells (FDCs)[23–25]. Retropharyngeal lymph node dendritic cells (CD45RO$^-$CD58$^+$) from three of three scrapie-infected sheep displayed Tyr-Tyr-Arg surface immunoreactivity with the monoclonal antibody 9A4 (8–29% of cells), but not the 4E4 isotype-control monoclonal antibody (0–0.4%), whereas similar cells from three uninfected sheep did not stain with either monoclonal antibody (Fig. 4c). No significant Tyr-Tyr-Arg surface immunoreactivity was observed on sheep or rodent lymphocytes, or on dissociated brain cells from end-stage ME7 scrapie-infected mice (data not shown), suggesting that FDCs may selectively accumulate cell-surface PrP^{Sc}.

DISCUSSION

We believe that the Tyr-Tyr-Arg motif constitutes the first hypothesis-driven PrP^{Sc}-selective epitope derived from consideration of isoform-selective antibody accessibility to amino-acid side chains exposed during conformational conversion in prion diseases. Tyr-Tyr-Arg antibodies, in addition to recognizing the protease-resistant PrP that is key to most current diagnostic tests for prion infection, can also recognize misfolded but protease-sensitive PrP (Figs. 2d and 3c and data not shown). In prion disease, the latter, newly recognized molecular species[26] is characteristic of certain prion strains[27], early prion infection[20–22] and interspecies prion transmission[28]. Protease-sensitive PrP^{Sc} may represent a transient intermediate between normal structure and the abnormal, misfolded and aggregated PrP isoform that has acquired protease resistance[29]. The population of misfolded protease-sensitive molecules may also contain PrP*, the hypothetical PrP isoform responsible for the property of prion infectivity[30].

We showed surface immunoreactivity for Tyr-Tyr-Arg on living dendritic cells from scrapie-infected sheep lymph nodes, suggesting that PrP^{Sc} can be maintained in the native (infectious) conformation on these cells. FDCs are implicated in the immune presentation to B cells of native-structure antigens, complexed at the cell surface with antibody or complement or both[31]. Recent studies have shown a role for complement components[32,33] and B cells[34] in lymphoid replication and subsequent neuroinvasion of prions. It is thus possible that native PrP^{Sc}, perhaps complexed with complement, may accumulate on FDCs for immune presentation to other lymphoid cells, which become concurrently infected with prions. Immune presentation of PrP^{Sc} must be ineffectual, as no antiprion humoral or cellular immune response has been detected in prion infection[35].

The PrP^{Sc}-selective Tyr-Tyr-Arg epitope may prove useful in immunotherapy or immunoprophylaxis of prion diseases. Recent findings show that antibodies directed predominantly against PrP^C can clear scrapie-infected cells of PrP^{Sc} in vitro[36,37] and can block the propagation of experimental scrapie in transgenic mice in vivo[9]. However, autoimmune recognition of PrP^C could cause inappropriate activation of signaling cascades[38], immunosuppression[39] and widespread complement-dependent cellular lysis[40], although in some experimental paradigms such antibodies are apparently toler-

ated[9,41]. Considering the key role of dendritic cells in scrapie, BSE and variant CJD[23,24,25], and the immunologic recognition of dendritic cell-surface PrP^{Sc} by Tyr-Tyr-Arg antibodies in physiological buffers (Fig. 4c), it is conceivable that circulating Tyr-Tyr-Arg antibodies could block prion neuroinvasion by neutralizing or opsonizing gut or lymphoid prions during the peripheral incubation phase of these diseases.

The isoform-selective exposure of Tyr-Tyr-Arg may help determine the structure of PrP^{Sc}, for which only low-resolution fragmentary structures are currently available[42]. The three Tyr-Tyr-X motifs of PrP are apparently obscured to antibody recognition in PrP^C by tertiary structural elements[14–16] and native post-translational modifications. We believe that the best candidate for the PrP^{Sc}-selective epitope is the Tyr-Tyr-Arg motif located in the PrP^C β-strand 2. In support of this idea, Tyr-Tyr-Arg monoclonal antibody binding is not inhibited by 6H4 antibody (recognizing an overlapping epitope in α-helix 1; ref. 7), Tyr-Tyr-Arg monoclonal antibody binding seems to be critically dependent on the terminal arginine residue (lacking in the Tyr-Tyr-Gln and Tyr-Tyr-Asp sequences of α-helix 3), and antibody access to the C terminus of native PrP (α-helix 3) does not differ for PrP^C and PrP^{Sc} (ref. 43). Moreover, considering that access to all three side chains is necessary for Tyr-Tyr-Arg antibody binding, we speculate that β-strand 2 becomes exposed in disease as a result of the dissolution of the short β-sheet of PrP^C. This notion is consistent with experimental data indicating that PrP^{Sc} has features of a molten globule[12,44] lacking some of the tertiary structural elements of PrP^C.

The prion diseases may provide a prototype for disorders of protein misfolding, including Alzheimer disease, amyotrophic lateral sclerosis and Parkinson disease. We hypothesize that conformational conversion of proteins in disease is accompanied by molecular surface exposure of previously sequestered amino-acid side chains. It is possible that exploitation of this 'side-chain accessibility' hypothesis, applied here to isoform-selective antibodies for PrP, may provide new diagnostic and therapeutic approaches to other post-translational disorders of the proteome.

METHODS

Tyrosine and tryptophan fluorescence at varying pH. Recombinant mouse PrP(23–231) (400 nM; gift of K. Qin and D. Westaway, University of Toronto) dissolved in 1.5 M guanidine hydrochloride (Sigma), 2 mM sodium phosphate (Sigma) and 2 mM sodium citrate (Sigma) buffers was monitored by steady-state fluorescence using a 2 nm bandpass. The excitation and emission wavelengths were 275 nm and 310 nm for tyrosine fluorescence and 293 nm and 350 nm for tryptophan fluorescence measurements, respectively.

Acrylamide quenching of tyrosine fluorescence. PrP(23–231) (400 nM) in 1.5 M guanidine hydrochloride, 2 mM sodium phosphate and 2 mM sodium citrate was titrated with increasing concentrations of acrylamide (Sigma) at pH values of 7 and 3. Tyrosine fluorescence was measured using an excitation wavelength of 275 nm (bandpass of 2 nm) and an emission wavelength of 311 nm (bandpass of 7 nm). Stern-Volmer plots were obtained by plotting the ratio of the observed fluorescence in the absence of acrylamide to the fluorescence in the presence of acrylamide.

Antibody generation. Polyclonal antibody C2 was produced by immunizing rabbits with KLH-conjugated Cys-Tyr-Tyr-Arg peptide. IgG from sera were purified on a protein A–Sepharose column (Pharmacia Amersham). Monoclonal antibodies were developed by immunizing and thrice boosting mice with KLH-conjugated CYYRRYYRYY peptide, in Freund complete adjuvant. Initial screening was done by testing antibody reactivity on 4-MAP-Tyr-Tyr-Arg–coated plates. Positive IgM was purified by size fractionation from ascites fluid. Monoclonal antibody variable regions were cloned into a

dog IgG framework from cDNA produced from hybridomas by PCR amplification. Light- and heavy-chain variable regions were amplified using forward primers specific to the leader sequences and reverse primers specific to the first exon of the constant regions. Dog light- and heavy-chain constant regions were amplified in a similar fashion. PCR products were annealed and amplified using primers specific to the outer ends. Overlapped light- and heavy-chain PCR fragments were cloned into pcDNA3 vectors. Plasmid DNA was transfected into 293 cells, at a 3:1 light-to-heavy chain molar ratio, using Lipofectamin2000 (Invitrogen) under standard conditions. Recombinant chimeric IgGs were purified on protein A–Sepharose. A polyclonal nondistinguishing antibody against PrP was produced by immunizing rabbits with a peptide corresponding to residues 23–56 of bovine PrP. IgG was purified from sera as described above.

Preparation of acidic guanidine-HCl–treated PrP. We mixed 100 µl of 10% brain homogenate with an equal volume of 3.0 M guanidine HCl (final concentration 1.5 M) in PBS at pH 7.4 or pH 3.5 adjusted with 1 N HCl, followed by incubation at room temperature with shaking. After 5 h, samples were mixed with five volumes of prechilled methanol and incubated at –20 °C for 2 h to precipitate the proteins. The samples were subjected to centrifugation at 16,000 g for 20 min at 4 °C to remove the acidic buffer and guanidine HCl, and pellets were resuspended in 100 µl of lysis buffer. The samples treated at pH 7.4 were designated as mock-treated samples.

Peptide ELISA. Hybridoma supernatants were produced by culturing hybridoma cells in DMEM (Wisent) supplemented with 20% FBS (Wisent). The culture medium was separated from the cells by centrifugation (1,000 g) for 10 min. Supernatants were diluted one-third in medium with 10% FCS and incubated with the indicated 4-MAP-peptide conjugates at 1 mg/ml final concentration for 2 h at 20–24 °C. Immulon-4 96-well plates (Dynex) were coated with 100 µl of peptide diluted to 10 µg/ml in 100 mM carbonate buffer (pH 9.6). The coated plates were blocked with PBS and 1% BSA (Sigma) for 2 h at room temperature. The supernatant mixtures were added to the 4-MAP-Tyr-Tyr-Arg–coated plates for 30 min. After 6–8 washes with PBS and 0.5% Tween 20, bound antibody was revealed using a horseradish peroxidase–labeled goat antibody to mouse immunoglobulin, diluted 1:3,000.

Bead ELISA. Five microliters of mouse 10% brain homogenates were incubated with 15 µl of magnetic bead-conjugated antibodies to Tyr-Tyr-Arg in 0.2 ml of immunoprecipitation binding buffer for 2 h at 20–24 °C with shaking. Washes were done in a similar fashion to the usual immunoprecipitation. Captured PrP^{Sc} was detected with purified rabbit IgG to PrP, followed by horseradish peroxidase–labeled donkey antibody to rabbit immunoglobulin (Jackson), diluted 1:1,000.

Flow cytometry. Fresh retropharyngeal lymph nodes from normal and scrapie-infected sheep were processed as modified from ref. 45. The tissue was dissected into small chunks and incubated three times, at 37 °C for 15 min, with a solution containing 0.15 mg/ml Blenzyme I (Roche Diagnostics) and 0.03 mg/ml DNase I (Roche Diagnostics). Viable lymph node cells were sequentially incubated for 15 min on ice with normal mouse serum, antibody to sheep CD58 (VMRD, Inc.), phycoerythrin-conjugated goat antibody to mouse IgG1 (Southern Biotech Associates), antibody to sheep CD45RO (VMRD, Inc.), biotin-conjugated goat antibody to mouse IgG3 (Southern Biotech Associates), phycoerythrin-Cy5–conjugated streptavidin (Serotec) and 10 µg/ml of either a PrP^{Sc}-specific antibody or the isotype control, followed by FITC-conjugated goat antibody to mouse IgM (Southern Biotech Associates). All antibody dilutions and washes were done using Dulbecco PBS supplemented with 2.5% FBS.

Note: Supplementary information is available on the Nature Medicine website.

1. Prusiner, S.B. Prions. *Proc. Natl. Acad. Sci. USA* 95, 13363–13383 (1998).
2. Will, R.G. *et al.* A new variant of Creutzfeldt-Jakob disease in the UK. *Lancet* 347, 921–925 (1996).
3. Coulthart, M.B. & Cashman, N.R. Variant Creutzfeldt-Jakob disease: a summary of current scientific knowledge in relation to public health. *Can. Med. Assoc. J.* 165, 51–58 (2001).
4. Bolton, D.C., McKinley M.P. & Prusiner S.B. Identification of a protein that purifies with the scrapie prion. Science 218, 1309–1311 (1982).
5. Pan, K.-M. *et al.* Conversion of alpha-helices into beta-sheets features in the formation of the scrapie prion proteins. *Proc. Natl. Acad. Sci. USA* 90, 10962–10966 (1993).
6. Pergami, P., Jaffe, H. & Safar, J. Semipreparative chromatographic method to purify the normal cellular isoform of the prion protein in nondenatured form. *Anal. Biochem.* 236, 63–73 (1996).
7. Korth, C. *et al.* Prion (PrP^{Sc})-specific epitope defined by a monoclonal antibody. *Nature* 390, 74–77 (1997).
8. Fischer, M.B., Roeckl, C., Parizek, P., Schwarz, H.P. & Aguzzi, A. Binding of disease-associated prion protein to plasminogen. *Nature* 408, 479–483 (2000).
9. Heppner, F.L. *et al.* Prevention of scrapie pathogenesis by transgenic expression of anti-prion protein antibodies. *Science* 294, 178–182 (2001).
10. Swietnicki, W., Petersen, R., Gambetti, P. & Surewicz, W.K. pH-dependent stability and conformation of the recombinant human prion protein PrP(90-231). *J. Biol. Chem.* 272, 27517–27520 (1997).
11. Hornemann, S. & Glockshuber, R. A scrapie-like unfolding intermediate of the prion protein domain PrP(121-231) induced by acidic pH. *Proc. Natl. Acad. Sci. USA* 95, 6010–6014 (1998).
12. Jackson, G.S. *et al.* Reversible conversion of monomeric human prion protein between native and fibrillogenic conformations. *Science* 283, 1935–1937 (1999).
13. Cioni, P. Oxygen and acrylamide quenching of protein phosphorescence: correlation with protein dynamics. Biophys. Chem. 87, 15–24 (2000).
14. Riek, R. *et al.* NMR structure of the mouse prion protein domain PrP(121-321). *Nature* 382, 180–182 (1996).
15. Liu, H. *et al.* Solution structure of Syrian hamster prion protein recombinant PrP(90-231). Biochemistry 38, 5362–5377 (1999).
16. Zahn, R. *et al.* NMR solution structure of the human prion protein. *Proc. Natl. Acad. Sci. USA* 97, 145–150 (2000).
17. Tang, L., Sampson, C., Dreitz, M.J. & McCall, C. Cloning and characterization of cDNAs encoding four different canine immunoglobulin gamma chains. *Vet. Immunol. Immunopathol.* 80, 259–270 (2001).
18. Selz, M., Mozes, L., Zismar, L. Muszkat, K.A. & Schechter, B. A tale of two peptides, TyrTyrGluGlu and TyrGluTyrGlu, and their diverse immune behaviour. *Behring Inst. Mitt.* 91, 54–66 (1992).
19. Zou, W-Q. & Cashman N.R. Acidic pH and detergents enhance *in vitro* conversion of human brain PrP^C to a PrP^{Sc}-like form. *J. Biol. Chem.* 277, 43942–43947 (2002).
20. Rubenstein, R. *et al.* Scrapie-infected spleens: analysis of infectivity, scrapie-associated fibrils, and protease-resistant proteins. *J. Infect. Dis.* 164, 29–35 (1991).
21. Race, R.E. & Ernst, D. Detection of proteinase K-resistant prion protein and infectivity in mouse spleen by 2 weeks after scrapie agent inoculation. *J. Gen. Virol.* 73, 3319–3323 (1992).
22. Tatzelt, J., Groth, D.F., Torchia, M., Prusiner, S.B. & DeArmond, S.J. Kinetics of prion protein accumulation in the CNS of mice with experimental scrapie. *J. Neuropathol. Exp. Neurol.* 58, 1244–1249 (1999).
23. Lezmi, S., Bencsik, A. & Baron, T. CNA42 monoclonal antibody identifies FDC as PrPsc accumulating cells in the spleen of scrapie affected sheep. *Vet. Immunol. Immunopathol.* 82, 1–8 (2001).
24. Hill, A.F. *et al.* Investigation of variant Creutzfeldt-Jakob disease and other human prion diseases with tonsil biopsy samples. *Lancet* 353, 183–189 (1999).
25. Mabbot, N.A. & Bruce M.E. The immunobiology of TSE diseases. *J. Gen. Virol.* 82, 2307–2318 (2001).
26. Safar, J.G. *et al.* Measuring prions causing bovine spongiform encephalopathy or chronic wasting disease by immunoassays and transgenic mice. *Nat. Biotechnol.* 20, 1147–1150 (2002).
27. Safar, J.G. *et al.* Eight prion strains have PrP(Sc) molecules with different conformations. *Nat. Med.* 4, 1157–1165 (1998).
28. Hill A.F. *et al.* Species-barrier-independent prion replication in apparently resistant

species. *Proc. Natl. Acad. Sci. USA* 97, 10248–10253 (2000).

29. Horiuchi M., Priola S.A., Chabry J. & Caughey B. Interactions between heterologous forms of prion protein:binding, inhibition of conversion, and species barriers. *Proc. Natl Acad. Sci. USA* 97, 5836–5841 (2000).

30. Aguzzi A. & Weissmann C. Prion research: the next frontiers. *Nature* 389, 795–798 (1997).

31. Szakal, A.K. & Tew, J.G. Follicular dendritic cells: B-cell proliferation and maturation. *Cancer Res.* 52, 5554s–5556s (1992).

32. Klein, M.A. *et al.* Complement facilitates early prion pathogenesis. *Nat. Med.* 7, 488–492 (2001).

33. Mabbott, N.A. *et al.* Temporary depletion of complement component C3 or genetic deficiency of C1q significantly delays onset of scrapie. *Nat. Med.* 7, 485–487 (2001).

34. Klein, M.A. *et al.* A crucial role for B cells in neuroinvasive scrapie. *Nature* 390, 687–690 (1997).

35. Gajdusek, D.C. Unconventional viruses causing subacute spongiform encephalopathies. in Virology (ed. Fields, B.N.) 1516–1557 (Raven Press, New York, 1986).

36. Enari, M., Flechsig, E. & Weissmann, C. Scrapie prion protein accumulation by scrapie-infected neuroblastoma cells abrogated by exposure to a prion protein antibody. *Proc. Natl. Acad. Sci. USA* 98, 9295–9299 (2001).

37. Peretz, D. *et al.* Antibodies inhibit prion propagation and clear cell cultures of prion infectivity. *Nature* 412, 739–743 (2001).

38. Mouillet-Richard, S. *et al.* Signal transduction through prion protein. *Science* 289, 1925–1928 (2000).

39. Cashman, N.R. *et al.* Cellular isoform of the scrapie agent protein participates in lymphocyte activation. *Cell* 61, 185–192 (1990).

40. Bendheim, P.E. *et al.* Nearly ubiquitous tissue distribution of the scrapie agent precursor protein. *Neurology* 42, 149–156 (1992).

41. White, A.R. *et al.* Monoclonal antibodies inhibit prion replication and delay the development of prion disease. *Nature* 422, 80–83 (2003).

42. Wille, H. *et al.* Structural studies of the scrapie prion protein by electron crystallography. *Proc. Natl. Acad. Sci. USA* 99, 3563–3568 (2002).

43. Peretz, D. *et al.* A conformational transition at the N terminus of the prion protein features in formation of the scrapie isoform. *J. Mol. Biol.* 273, 614–622 (1997).

44. Safar, J., Roller, P.P., Gajdusek, D.C. & Gibbs, C.J. Jr. Scrapie amyloid (prion) protein has the conformational characteristics of an aggregated molten globule folding intermediate. *Biochemistry* 33, 8375–8383 (1994).

45. Szakal, A.K., Gieringer, R.L., Kosco, M.H & Tew J.G. Isolated follicular dendritic cells: cytochemical antigen localization, Nomarski, SEM, and TEM morphology. *J. Immunol.* 134, 1349–1359 (1985).

Pep #	Bovine aa	Bovine Sequence
1	25-37	KKRPKPGGGWNTG
2	27-39	RPKPGGGWNTGGS
3	29-41	KPGGGWNTGGSRY
4	31-43	GGGWNTGGSRYPG
5	33-45	GWNTGGSRYPGQG
6	35-47	NTGGSRYPGQGSP
7	37-49	GGSRYPGQGSPGG
8	39-51	SRYPGQGSPGGNR
9	41-53	YPGQGSPGGNRYP
10	43-55	GQGSPGGNRYPPQ
11	45-57	GSPGGNRYPPQGG
12	47-59	PGGNRYPPQGGGG
13	49-61	GNRYPPQGGGGWG
14	51-63	RYPPQGGGGWGQP
15	53-65	PPQGGGGWGQPHG
16	55-67	QGGGGWGQPHGGG
17	57-69	GGGWGQPHGGGWG
18	59-71	GWGQPHGGGWGQP
19	61-73	GQPHGGGWGQPHG
20	63-75	PHGGGWGQPHGGG
21	65-77	GGGWGQPHGGGWG
22	67-79	GWGQPHGGGWGQP
23	69-81	GQPHGGGWGQPHG
24	71-83	PHGGGWGQPHGGG
25	73-85	GGGWGQPHGGGWG
26	75-87	GWGQPHGGGWGQP
27	77-89	GQPHGGGWGQPHG
28	79-91	PHGGGWGQPHGGG
29	81-93	GGGWGQPHGGGWG
30	83-95	GWGQPHGGGWGQP
31	85-97	GQPHGGGWGQPHG
32	87-99	PHGGGWGQPHGGG
33	89-101	GGGWGQPHGGGGW
34	91-103	GWGQPHGGGGWGQ
35	93-105	GQPHGGGGWGQGG
36	95-107	PHGGGGWGQGGTH
37	97-109	GGGGWGQGGTHGQ
38	99-111	GGWGQGGTHGQWN
39	101-113	WGQGGTHGQWNKP
40	103-115	QGGTHGQWNKPSK
41	105-117	GTHGQWNKPSKPK
42	107-119	HGQWNKPSKPKTN
43	109-121	QWNKPSKPKTNIK

44	111-123	NKPSKPKTNIKHV
45	113-125	PSKPKTNIKHVAG
46	115-127	KPKTNIKHVAGAA
47	117-129	KTNIKHVAGAAAA
48	119-131	NIKHVAGAAAAGA
49	121-133	KHVAGAAAAGAVV
50	123-135	VAGAAAAGAVVGG
51	125-137	GAAAAGAVVGGLG
52	127-139	AAAGAVVGGLGGY
53	129-141	AGAVVGGLGGYML
54	131-143	AVVGGLGGYMLGS
55	133-145	VGGLGGYMLGSAM
56	135-147	GLGGYMLGSAMSR
57	137-149	GGYMLGSAMSRPL
58	139-151	YMLGSAMSRPLIH
59	141-153	LGSAMSRPLIHFG
60	143-155	SAMSRPLIHFGSD
61	145-157	MSRPLIHFGSDYE
62	147-159	RPLIHFGSDYEDR
63	149-161	LIHFGSDYEDRYY
64	151-163	HFGSDYEDRYYRE
65	153-165	GSDYEDRYYRENM
66	155-167	DYEDRYYRENMHR
67	157-169	EDRYYRENMHRYP
68	159-171	RYYRENMHRYPNQ
69	161-173	YRENMHRYPNQVY
70	163-175	ENMHRYPNQVYYR
71	165-177	MHRYPNQVYYRPV
72	167-179	RYPNQVYYRPVDQ
73	169-181	PNQVYYRPVDQYS
74	171-183	QVYYRPVDQYSNQ
75	173-185	YYRPVDQYSNQNN
76	175-187	RPVDQYSNQNNFV
77	177-189	VDQYSNQNNFVHD
78	179-191	QYSNQNNFVHDCV
79	181-193	SNQNNFVHDCVNI
80	183-195	QNNFVHDCVNITV
81	185-197	NFVHDCVNITVKE
82	187-199	VHDCVNITVKEHT
83	189-201	DCVNITVKEHTVT
84	191-203	VNITVKEHTVTTT
85	193-205	ITVKEHTVTTTTK
86	195-207	VKEHTVTTTTKGE
87	197-209	EHTVTTTTKGENF
88	199-211	TVTTTTKGENFTE
89	201-213	TTTTKGENFTETD
90	203-215	TTKGENFTETDIK

91	205-217	KGENFTETDIKMM
92	207-219	ENFTETDIKMMER
93	209-221	FTETDIKMMERVV
94	211-223	ETDIKMMERVVEQ
95	213-225	DIKMMERVVEQMC
96	215-227	KMMERVVEQMCIT
97	217-229	MERVVEQMCITQY
98	219-231	RVVEQMCITQYQR
99	221-233	VEQMCITQYQRES
100	223-235	QMCITQYQRESQA
101	225-237	CITQYQRESQAYY
102	227-239	TQYQRESQAYYQR
103	229-241	YQRESQAYYQRGA
104	231-243	RESQAYYQRGASV